

# Experimental and Theoretical Investigation of Vibrational Overtones of Glycolic Acid and Its Hydrogen Bonding Interactions with Water

Daniel K. Havey,<sup>†</sup> Karl J. Feierabend,<sup>†</sup> Kaito Takahashi,<sup>‡</sup> Rex T. Skodje,<sup>†,‡</sup> and Veronica Vaida<sup>\*,†</sup>

Department of Chemistry and Biochemistry and CIRES, University of Colorado, Campus Box 215, Boulder, Colorado 80309, and Institute of Atomic and Molecular Physics, Academia Sinica, P.O. Box 23-166, Taipei, Taiwan

Received: January 27, 2006; In Final Form: March 23, 2006

The present work reports observations of the  $4\nu_1$  and  $4\nu_2$  O–H stretching transitions in glycolic acid, CH<sub>2</sub>OHCOOH, using a highly sensitive cavity ring-down spectrometer. Experimental and theoretical values for the harmonic frequencies and anharmonic constants of both O–H stretching transitions were extracted and are compared with theoretical calculations in the literature. Calculations of anharmonic frequencies, intensities, and relative energies have been performed and are presented for three conformers of glycolic acid. In the presence of water, an interesting broad spectral feature appeared underneath  $4\nu_1$  and  $4\nu_2$ . New calculations for harmonic frequencies, intensities, and relative energies of four CH<sub>2</sub>OHCOOH–H<sub>2</sub>O complexes are reported to aid in understanding the observed spectrum. This work suggests that the perturbations are caused by intermolecular hydrogen bonding of glycolic acid with one or more water molecules.

## Introduction

The issues of interest in this study are hydrogen-bonding interactions in glycolic acid (CH<sub>2</sub>OHCOOH). Glycolic acid is an interesting system in this regard because it offers the opportunity to study both intra- and intermolecular hydrogen bonding. Vibrational spectra of this molecule have been studied using experimental and theoretical methods, yet these studies have been limited by spectral overlap of the two O–H stretches.<sup>1,2</sup> Specifically, the  $\nu_1$  and  $\nu_2$  normal modes (where  $\nu_1$  is the acid O–H stretching mode and  $\nu_2$  is the alcohol O–H stretching mode) coincidentally occur at the same frequency in both the fundamental and first overtone regions. The nature of the two O–H stretching transitions is interesting because the alcohol O–H stretch exhibits intramolecular hydrogen bonding<sup>2</sup> while the O–H stretch of the acid is available for intermolecular hydrogen bonding.<sup>3,4</sup> Thus, CH<sub>2</sub>OHCOOH is an intriguing prototype system for understanding perturbations to vibrational spectra of organic acids from intra- and intermolecular interactions.

Previous work on glycolic acid has focused on its matrix and near-IR spectroscopy<sup>1,2</sup> as well as several studies on the energetics of its conformers.<sup>2,5,6</sup> The microwave spectrum of gas-phase glycolic acid has also been published and continues to aid in understanding the structure of this molecule.<sup>6,7</sup> Because of glycolic acid's low vapor pressure ( $\sim 101$  Pa at 373 K<sup>8</sup>), its gas-phase spectroscopy was not investigated until recently.<sup>1</sup> Also, the structures of glycolic acid hydrogen bonded to up to six water molecules have been studied using ab initio theoretical methods.<sup>3,4</sup> However, evidence of hydrogen bond formation has not been experimentally obtained.

This work is also motivated by the interest in understanding the importance of organic molecules in atmospheric chemistry

and climate. Glycolic acid makes up a significant portion of the organic content of ( $\sim 2$ – $5\%$  in a polluted troposphere) atmospheric aerosols<sup>9</sup> in part due to its strong tendency toward intermolecular hydrogen bonding (e.g., with water). It also makes up a larger family of organic acids that have recently been discussed in terms of their connection to both atmospheric chemistry and spectroscopy.<sup>10</sup> Recent studies have built on previous spectroscopic and theoretical work on X–H stretching overtones.<sup>11–20</sup> Specifically, atmospheric excitation of vibrational overtones via solar photons has been studied in relation to overtone-induced photodissociation.<sup>15,21–28</sup> Fundamental spectroscopic studies of molecules such as glycolic acid help to provide a broader knowledge base to understand vibrational overtones and vibrationally mediated chemical reactions.

Prior to this work, the highest energy vibrational transitions observed for glycolic acid were the overlapping  $2\nu_1$  and  $2\nu_2$  O–H stretching first overtones. It was predicted<sup>1</sup> that examining these transitions at higher energies might separate them. This separation is complicated by the fact that higher overtones typically become less intense by about an order of magnitude for each successive transition.<sup>11</sup> Observation of higher energy transitions by conventional methods (FTIR) is difficult due to sensitivity limitations. The present work uses a highly sensitive cavity ring-down spectrometer to observe the  $4\nu_1$  and  $4\nu_2$  transitions in glycolic acid. Both transitions were observed under dry conditions in which water impurities have been removed by vacuum sublimation. Experimental and theoretical values for the harmonic frequencies and anharmonic constants of both O–H stretching transitions were extracted and are compared with theoretical calculations in the literature. Also, new calculations for anharmonic frequencies, intensities, and relative energies are presented for three conformers of glycolic acid. In the presence of water, an interesting broad spectral feature appeared underneath  $4\nu_1$  and  $4\nu_2$ . New calculations for harmonic frequencies, intensities, and relative energies of four CH<sub>2</sub>OHCOOH–H<sub>2</sub>O complexes are reported and are used to help

\* To whom correspondence should be addressed. E-mail: vaida@colorado.edu.

<sup>†</sup> University of Colorado.

<sup>‡</sup> Institute of Atomic and Molecular Physics.

explain spectral perturbations. This work suggests that the perturbations are caused by intermolecular hydrogen bonding of glycolic acid with water. Observation of such features may have broader implications for the study of hydrogen-bonded molecular clusters, which may be significant contributors to atmospheric chemistry and climate.<sup>29–31</sup>

### Experimental Section

Spectra of glycolic acid were taken using a pulsed cavity ring-down spectrometer very similar to that of Brown et al.<sup>28</sup> The cell was wrapped with heating tape, insulating cotton, and aluminum foil, allowing for temperature control. The heating system was calibrated by inserting a thermocouple into the cell and monitoring the internal temperature under the same conditions as those used in the experiment. Glycolic acid vapor was prepared by heating a solid reservoir of Aldrich 99 wt % CH<sub>2</sub>OHCOOH to 365 ± 2.5 K and flowing 0.0–1.0 slpm of He gas at a constant rate over the top of the sample. The effective path length of the cell ( $R_L$ ) is the ratio of the distance between the cavity mirrors and the distance over which the sample is present and was 1.2 ± 0.2 for these experiments. Two different solid samples were used during these experiments. The first is a “wet” sample in which the glycolic acid was put in a solid reservoir as obtained from the manufacturer (99 wt % has a primary impurity of H<sub>2</sub>O). The second is a “dry” sample in which the glycolic acid had undergone vacuum sublimation<sup>1,7</sup> for 12 h at 363 ± 5 K. All experiments were performed at constant flow rates at atmospheric pressure.

Glycolic acid vapor is difficult to observe spectroscopically primarily due to its low vapor pressure (~30.3 Pa at 348 K and ~101 Pa at 373 K). In addition, under the conditions of the present study, the wet glycolic acid sample readily formed aerosols at temperatures greater than 383 K, preventing any ring-down signal from being obtained (ring-down time constants decreased to <5 μs). At even higher temperatures, glycolic acid is known to thermally decompose into CO, H<sub>2</sub>O, and CH<sub>2</sub>O.<sup>32</sup> Glycolic acid can dimerize at lower temperatures, which is an effect common to organic acids, such as acetic acid, for example.<sup>33</sup> These problems severely restrict the temperature range over which experimental spectra can be collected. Thus, to maximize the number density of the glycolic acid monomer and prevent aerosol formation in the wet sample, the cell was maintained at 365 ± 2.5 K. This allowed enough CH<sub>2</sub>OHCOOH vapor in the cell to observe 4ν<sub>1</sub> and 4ν<sub>2</sub>. No features due to the glycolic acid dimer were observed. Spectra were collected over several days to ensure consistency in the results.

High reflectivity mirrors were connected to the cell with a peak reflectivity at 760 nm. The mirrors used for observation of 4ν<sub>1</sub> and 4ν<sub>2</sub> had a 1 m radius of curvature and gave a maximum observable ring-down time constant of 128 μs at 750 nm ( $R > 99.997\%$ ). Condensation on the mirrors was prevented using a purge volume of helium next to both mirrors as discussed below. Mirror cleanliness was monitored carefully over the course of these experiments. With the cell maintained at 365 ± 2.5 K, there was no noticeable change in the maximum observable ring-down time constant over the course of the experiments.

Each mirror was connected to a mount made up of an adjustable flange connected to a fixed flange by steel bellows, similar to the apparatus of Atkinson et al.<sup>34</sup> Alignment of the mirrors was obtained by supporting the mirror mounts inside of commercial kinematic adjusters. A small purge volume of helium was introduced directly in front of the mirrors at a constant flow rate of 0.5 slpm through 1/4 in. diameter ports.

The light source used for the absorption experiments was a Northern Lights tunable dye laser (NL-5-2 MF6) pumped by a Big Sky frequency doubled Nd:YAG laser. The wavelength of the dye laser was calibrated using a 0.01 nm resolution spectrum of H<sub>2</sub>O at 434 K over the region (730–740 nm).<sup>35</sup> The bandwidth of the dye laser was estimated to be a maximum of 1 cm<sup>-1</sup> according to the manufacturer's specifications. Nonexponential ring-down decays were observed for water since the dye laser bandwidth was greater than the line width of its transitions. However, this effect is insignificant since the calibration was only concerned with the frequencies for H<sub>2</sub>O. The pulse width of the Nd:YAG laser had a full-width at half-maximum (fwhm) of 7 ns. The LDS 751 laser dye was chosen (max pulse energy of 1.6 mJ at 744 nm, tuning range of approximately 725 to 780 nm, 3 × 10<sup>-4</sup> M) to best overlap the predicted overtone transitions in glycolic acid. The output from the dye laser was directed through an isolator composed of a polarizer (Newport, 10GLO8AR.14) and waveplate (Newport, 05RP). The beam passed through a 50 cm focal length lens to collimate the beam to a spot size similar to the low-order transverse electric modes of the optical resonator. The beam was then directed to two turning mirrors before entering the previously described cell. The residual beam exiting the cell was directed onto a turning mirror and through a negative lens of focal length 50 cm where it was expanded onto a commercial PMT (Hamamatsu, R943-02), interfaced to a commercially available data acquisition card (Gage Compuscope 1250). The interfaced software has been described previously in the literature.<sup>28</sup> The card sampled at 2 MHz for all experiments. In the spectral regions of interest, 10 ring-downs were averaged per wavelength interval with resolutions of 0.2 and 0.01 nm. Under the conditions for these experiments, the minimum detectable absorption coefficient was calculated to be 5 × 10<sup>-10</sup> cm<sup>-1</sup> for a 1 s integration time.<sup>36</sup>

### Theory and Calculations

The structures of the three stable conformers of glycolic acid and their monohydrated complex, CH<sub>2</sub>OHCOOH–H<sub>2</sub>O, were calculated using the hybrid density functional theory method using the B3LYP<sup>37,38</sup> functional with the 6-311++G(3df,-3pd)<sup>39–43</sup> basis set on the Gaussian 03 program.<sup>41</sup> The harmonic zero-point vibrational energies were calculated at the respective equilibrium geometries and added to the electronic energy for comparison in the relative energy difference between the different conformers. For glycolic acid, the potential energy curve and the dipole moment function, used for the local mode vibrational calculation, were obtained by varying the OH bond length while keeping all other structural parameters fixed at their equilibrium values.

In the local mode vibrational calculation,<sup>16–18</sup> we solve the Schrodinger equation for the one-dimensional molecular vibration

$$\left[ -\frac{\hbar^2}{2m} \frac{d^2}{dR^2} + V(R) \right] \psi_v(R) = E_v \psi_v(R) \quad (1)$$

where  $R$ ,  $m$ , and  $V(R)$  are the internuclear distance, the reduced mass, and the potential energy curve, respectively. The integrated absorption coefficient (cm molecule<sup>-1</sup>) of each OH stretching transition is given by

$$A(\nu) = \frac{8\pi^3}{3hc} |\langle \psi_v | \vec{\mu} | \psi_0 \rangle|^2 \tilde{\nu}_{\nu 0} \quad (2)$$

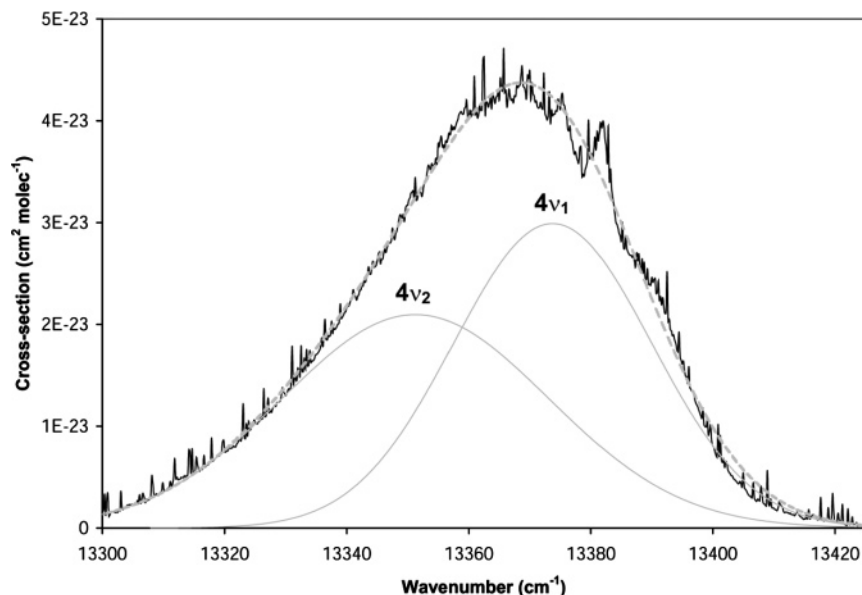


**Figure 1.** Cavity ring-down spectrum of glycolic acid under dry conditions at  $365 \pm 2.5$  K and 0.01 nm resolution. The solid gray traces show the two mixed Gaussian/Lorentzian functions used to simulate the two transitions in the spectrum. The dashed gray trace shows the sum of the two functions (goodness of fit,  $\chi^2 = 0.763$ ). The parameters for each peak are  $4\nu_1$  at  $13373 \text{ cm}^{-1}$ ,  $\text{fwhm} = 38 \text{ cm}^{-1}$ ;  $4\nu_2$  at  $13351 \text{ cm}^{-1}$ ,  $\text{fwhm} = 42 \text{ cm}^{-1}$ . The total integrated cross-section for the combined  $4\nu_1$  and  $4\nu_2$  transitions is approximately  $3.1 \times 10^{-21} \text{ cm molecule}^{-1}$ .

where  $\tilde{\nu}_{v_0}$  is the transition energy ( $E_v - E_0$ ) in  $\text{cm}^{-1}$  and  $|\langle \psi_v | \vec{\mu} | \psi_0 \rangle|^2$  is the square of the transition moment vector. The vibrational calculation was done on the *Mathematica* program using the grid variational method as reported before by one of the authors.<sup>44,45</sup>

## Results and Discussion

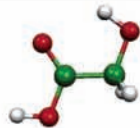
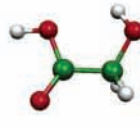
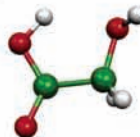
In Figure 1, a portion of the spectrum obtained for dry glycolic acid using the cavity ring-down spectrometer is shown. The  $4\nu_1$  and  $4\nu_2$  transitions are distinguishable. The spectrum contains overlapping absorbance due to these two vibrational transitions which are separating because of different harmonic frequencies and anharmonicities. This separation is evidenced by the fwhm of the feature being  $60 \text{ cm}^{-1}$  which is an increase of about a factor of 2 in the fwhm of  $\nu_1/\nu_2$  and  $2\nu_1/2\nu_2$ .<sup>1</sup> An attempt was made to model the rotational envelopes of the alcohol and overtone transitions using a standard asymmetric top Hamiltonian, but a reproduction of the observed band shape proved too challenging given the uncertainties in the band origins, relative intensities, temperature, and upper-state rotational constants. Instead, the absorbance region was analyzed by modeling a convolution of  $4\nu_1/4\nu_2$  with two mixed Gaussian/Lorentzian functions. There is a distinct absorption feature on the high-energy side of the overlapping transitions in Figure 1. This spectral feature observed at  $13382 \pm 1 \text{ cm}^{-1}$  to high energy of the main peak was assigned as the Q-branch of the acid O–H stretch,  $4\nu_1$ . The band centers of both transitions were obtained by modeling the absorption profile with two mixed Gaussian/Lorentzian functions using standard nonlinear least-squares iterative fitting (see Figure 1 for results). This analysis allowed identification of the band center frequencies for  $4\nu_1$  and  $4\nu_2$  at  $13373 \pm 1$  and  $13351 \pm 1 \text{ cm}^{-1}$ , respectively. These acid and alcohol assignments are qualitatively justified by comparing  $4\nu_1$  for formic acid ( $\sim 13280 \text{ cm}^{-1}$ )<sup>46</sup> and  $4\nu_1$  for methanol ( $\sim 13700 \text{ cm}^{-1}$ )<sup>47</sup> which are the analogous acid and alcohol to glycolic acid. The intramolecular hydrogen bonding would substantially red shift the alcohol O–H stretching transition away from the  $\sim 13700 \text{ cm}^{-1}$  observed for the O–H

stretch in methanol, an effect that has been observed in the fundamental and first overtone regions.<sup>1</sup>

Experimental values for the total integrated cross-sections for  $4\nu_1$  and  $4\nu_2$  were obtained by integration of the observed features (Figure 1) over wavenumber. A number density of  $2.0 \times 10^{16} \text{ molecules cm}^{-3}$  was calculated from the vapor pressure of glycolic acid at 373 K, since this was the only available data.<sup>8</sup> This value should be close to the vapor pressure at 365 K. By the use of Beer's law, the integrated absorption cross-section for the transitions was found to be  $3.1 \times 10^{-21} \text{ cm/molecule}$ . Through the use of the theoretical prediction of the relative line intensities (see Table 1), the cross-section can be decomposed into a  $1.5 \times 10^{-21} \text{ cm/molecule}$  component for the  $4\nu_2$  alcohol O–H stretch and a  $1.6 \times 10^{-21} \text{ cm/molecule}$  component for the  $4\nu_1$  acid O–H stretch.

Table 1 also presents a compilation of new O–H stretching vibrational frequencies, intensities, and relative energies for the three lowest energy conformers of glycolic acid. Recent near-IR work had assigned a narrow feature to high energy of the  $\nu_1/\nu_2$  O–H stretches as attributed to the lowest energy rotational isomer of glycolic acid.<sup>1</sup> The assignment was based on previous matrix isolation spectroscopy,<sup>2</sup> harmonic frequency, and anharmonicity calculations, as well as Boltzmann statistics.<sup>1</sup> The Boltzmann population analysis assumes that the population of the rotational isomers is  $e^{-\Delta E/kT}$  where  $\Delta E$  is the difference of the zero-point corrected energies of the isomers. Calculations in the present work reaffirm this assignment in two ways. First, the frequencies calculated using B3LYP 6-311++G(3df,3pd) again qualitatively predict the acidic O–H stretch of the second lowest energy conformer ( $3596 \text{ cm}^{-1}$ ) to be higher in frequency than that of  $\nu_1$  of the lowest energy conformer ( $3593 \text{ cm}^{-1}$ ). Previous work had calculated  $3657$  and  $3582 \text{ cm}^{-1}$  for these two conformers, respectively.<sup>1</sup> Second, new calculated intensities in the present work agree favorably with the near-IR observations at  $353 \pm 5 \text{ K}$ .<sup>1</sup> Through the use of the zero-point corrected energies for the conformers presented in Table 1 as well as previous literature values,<sup>6</sup> the equilibrium distribution should consist of  $\leq 97.5\%$  of the lowest energy conformer at 353 K. Previous estimates<sup>2</sup> of the zero-point corrected energies likewise

**TABLE 1: Compilation of Density Functional Theory Calculations for Frequencies, Intensities, and Relative Energies of Glycolic Acid and Its Two Lowest Energy Rotational Isomers Using B3LYP 6-311++G(3df,3pd)**

Glycolic Acid Isomer 0.00 kcal/mol					
	$\nu_1$ Acid O-H Stretch		$\nu_2$ Alcohol O-H Stretch		
Quantum Number ( $\nu$ )	Anharmonic Frequency ( $\text{cm}^{-1}$ )	Intensity ( $\text{cm/molecule}$ )	Anharmonic Frequency ( $\text{cm}^{-1}$ )	Intensity ( $\text{cm/molecule}$ )	Structural Representation
1	3593	9.56E-18	3567	1.20E-17	 0.00 kcal/mol isomer
2	7027	5.94E-19	6965	3.01E-19	
3	10310	3.17E-20	10197	1.94E-20	
4	13445	2.41E-21	13271	1.66E-21	
5	16438	2.82E-22	16190	2.09E-22	
6	19293	4.52E-23	18963	3.64E-23	
Glycolic Acid Isomer 2.56 kcal/mol					
	$\nu_1$ Acid O-H Stretch		$\nu_2$ Alcohol O-H Stretch		
Quantum Number ( $\nu$ )	Anharmonic Frequency ( $\text{cm}^{-1}$ )	Intensity ( $\text{cm/molecule}$ )	Anharmonic Frequency ( $\text{cm}^{-1}$ )	Intensity ( $\text{cm/molecule}$ )	Structural Representation
1	3596	9.68E-18	3665	6.14E-18	 2.56 kcal/mol isomer
2	7034	5.45E-19	7171	3.90E-19	
3	10321	2.89E-20	10521	2.26E-20	
4	13460	2.21E-21	13723	1.78E-21	
5	16458	2.57E-22	16780	2.09E-22	
6	19318	4.09E-23	19697	3.24E-23	
Glycolic Acid Isomer 3.24 kcal/mol					
	$\nu_1$ Acid O-H Stretch		$\nu_2$ Alcohol O-H Stretch		
Quantum Number ( $\nu$ )	Anharmonic Frequency ( $\text{cm}^{-1}$ )	Intensity ( $\text{cm/molecule}$ )	Anharmonic Frequency ( $\text{cm}^{-1}$ )	Intensity ( $\text{cm/molecule}$ )	Structural Representation
1	3478	2.38E-17	3691	8.22E-18	 3.24 kcal/mol isomer
2	6779	3.76E-19	7221	5.90E-19	
3	9906	2.53E-20	10594	2.91E-20	
4	12864	2.42E-21	13814	2.04E-21	
5	15660	3.22E-22	16886	2.22E-22	
6	18300	5.58E-23	19813	3.27E-23	

**TABLE 2: Comparison of Observed and Calculated Frequencies for the Fundamental and Overtone Transitions of  $\nu_1$  and  $\nu_2$  in Glycolic Acid Vapor**

	experimental frequency (cm <sup>-1</sup> )	calculated frequency (cm <sup>-1</sup> ) B3LYP 6-311++G(3df,3pd) unscaled	calculated frequency (cm <sup>-1</sup> ) B3LYP 6-311++G(2d,2p) ref 1
$\nu_1$	3585.5, ref 1	3593	3581.7
$2\nu_1$	6995.6, ref 1	7027	6988.2
$4\nu_1$	$13382 \pm 2^a$	13445	13278
$\nu_2$	3585.5, ref 1	3567	3561.0
$2\nu_2$	6995.6, ref 1	6965	6942.8
$4\nu_2$	$13355 \pm 10^a$	13271	13168.8

<sup>a</sup> Present cavity ring-down work.

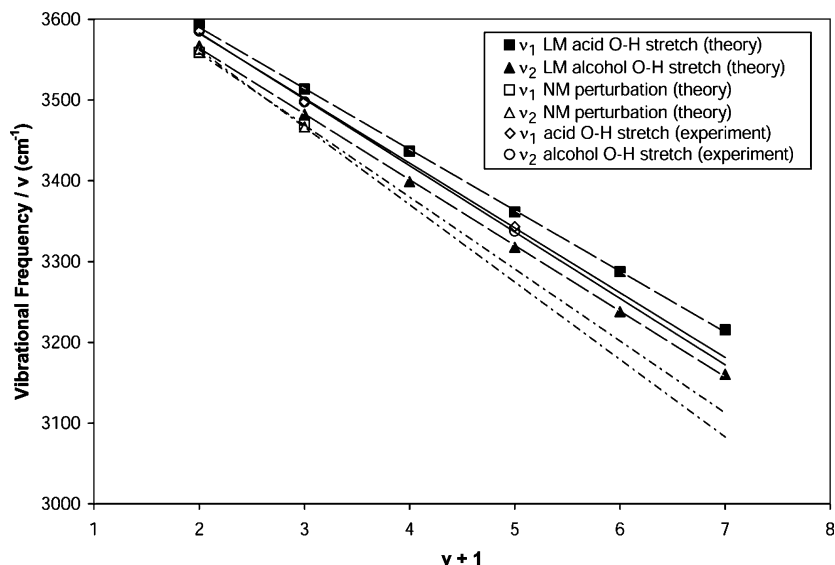


**Figure 2.** Birge–Sponer plot including linear fits for both  $\nu_1$  and  $\nu_2$  of glycolic acid. Theoretical values using the local mode (LM) and normal mode (NM) perturbation approaches are shown for comparison. Note the significantly smaller difference in frequency between the two modes in the case of the NM perturbation.

led us to believe the lowest conformer will dominate the distribution. If this is correlated with the new rotamer intensity calculations from Table 1, then one obtains that the vibrational spectrum in the IR/near-IR should have a contribution from the acid O–H stretch in the second lowest energy conformer which is 1–3% of the total  $\nu_1/\nu_2$  intensity. This is in excellent agreement with the observed  $2.1 \pm 1.2\%$  contribution which was attributed to absorption by the second lowest energy conformer.

Table 2 compares the calculated and experimental transition frequencies. Both sets of theoretical values predict the frequency of the alcohol O–H stretch ( $\nu_2$ ) to be less than that of the acid O–H stretch ( $\nu_1$ ). In addition, predicted frequencies for  $n\nu_1$  agree better with the experimental values than those for  $n\nu_2$ . The observation of the separating  $4\nu_1/4\nu_2$  transitions in the third overtone region is an important result, but the transitions did not separate as much as predicted by the calculations in previous near-IR work.<sup>1</sup> The near-IR work had observed both  $\nu_1/\nu_2$  and  $2\nu_1/2\nu_2$  in almost complete accidental degeneracy. However, high-resolution observations of two distinct sets of rotational lines had implied that the two transitions could be separated at higher energies where different anharmonicities would shift  $\nu_1$  and  $\nu_2$  by different amounts. Anharmonic frequency calculations from the present work predicted  $4\nu_1$  to occur at  $13\,445\text{ cm}^{-1}$  and the alcohol O–H stretch at  $13\,271\text{ cm}^{-1}$  (Table 1). The predicted separation of  $\sim 175\text{ cm}^{-1}$  is much greater than the  $\sim 20\text{--}25\text{ cm}^{-1}$  separation that was actually observed.

There are two possible explanations for this difference in splitting (1) the limitation of using the B3LYP method to calculate the potential energy curve or (2) the limitation in the

usage of the local mode model picture for the vibrational calculation. To gain a deeper understanding on this discrepancy, we performed further analysis on the most stable glycolic acid isomer. As Kjaergaard has reported,<sup>48</sup> B3LYP overestimates the red shift in a hydrogen-bonded stretch vibration; thus, theoretical values given for the O–H stretch vibrations may be overestimating the red shift. Local mode vibrational calculation using the potential energy curve calculated by the MP2 method with the same basis set resulted in a  $150\text{ cm}^{-1}$  splitting between the third overtone peaks. To examine the importance of the coupling with other vibrational modes, we performed anharmonic corrections to the harmonic normal mode frequencies using the perturbative scheme reported by Barone,<sup>49</sup> using the B3LYP potential energy surface. It was found that the vibrational coupling causes the splitting between the two O–H stretching modes to decrease at the first overtone level. Under the perturbative calculation, the separation between  $2\nu_1$  and  $2\nu_2$  is  $5\text{ cm}^{-1}$  while the local mode approximation (see Table 1) results in a  $60\text{ cm}^{-1}$  separation. The effect of the coupling is clearly seen in Figure 2, where a Birge–Sponer plot for the  $\nu_1$  and  $\nu_2$  modes of glycolic acid is given for the experimental and theoretical values. Interestingly, the O–H stretching mode showed a large coupling with the concerted O–H wagging motion. This wagging motion of the acidic and alcoholic O–H bonds is strongly coupled by the intramolecular hydrogen bond in this molecule, thus, resulting in a concerted wagging vibrational mode. Therefore, it is expected that vibrational coupling with other vibrational modes, especially the concerted O–H wagging vibration, is the probable origin for the discrepancy in the splitting between the local mode theoretical

**TABLE 3: Comparison of Experimentally Derived and Calculated Harmonic Frequencies and Anharmonic Constants**

	$\nu_1$ harmonic frequency (cm <sup>-1</sup> )	$\nu_1$ anharmonic constant (cm <sup>-1</sup> )	$\nu_2$ harmonic frequency (cm <sup>-1</sup> )	$\nu_2$ anharmonic constant (cm <sup>-1</sup> )
experimental <sup>a</sup>	3743.0	80.3	3747.7	82.2
calculated B3LYP 6-311++G(3df,3pd)	3741	75.5	3727	81.4

<sup>a</sup> Present cavity ring-down work.

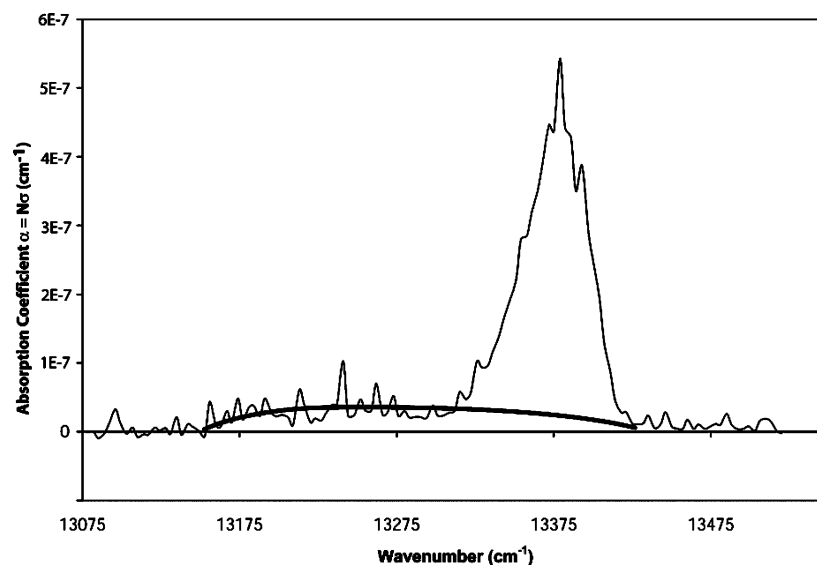


**Figure 3.** Spectrum of glycolic acid vapor obtained <36 Pa of H<sub>2</sub>O (wet conditions) at 365 ± 2.5 K and 0.2 nm resolution. The broad spectral feature between 13 150 and 13 600 cm<sup>-1</sup> is emphasized with the black trace and occurs only in the presence of water. This feature makes up ~4% of the total integrated intensity.

**TABLE 4: Compilation of New Density Functional Theory Calculations for Frequencies (harmonic), Intensities, Relative Energies, and Binding Energies of CH<sub>2</sub>OHCOOH–H<sub>2</sub>O and Three of Its Rotational Isomers Using B3LYP 6-311++G(3df,3pd)<sup>a</sup>**

Structural Representation				
ΔE, ZPE-corrected	0.00	3.339	2.208	6.949
ΔE <sup>b</sup> , ZPE-corrected	0.00	2.85	2.26	7.04
BE (ZPE-corrected)	9.317 (6.962)	6.020 (3.623)	9.682 (7.315)	5.462 (3.761)
Acid O-H Freq.	3337	3745	3315	3443
Acid O-H Int.	1.28E-16	1.05E-17	1.33E-16	1.29E-16
Alcohol O-H Freq.	3741	3595	3820	3828
Alcohol O-H Int.	1.24E-17	4.95E-17	9.18E-18	9.50E-18
H-Bond O-H Freq.	3673	3674	3641	3714
H-Bond O-H Int.	4.04E-17	7.67E-17	4.96E-17	3.05E-17
Free O-H Freq.	3876	3883	3876	3882
Free O-H Int.	1.64E-17	1.48E-17	1.54E-17	1.88E-17

<sup>a</sup> All energies are in kcal mol<sup>-1</sup>, frequencies in cm<sup>-1</sup>, and intensities in cm molecule<sup>-1</sup>. ZPE: zero-point energy; BE: binding energy.  
<sup>b</sup> Reference 4.

calculation and the experimental results. In addition, the relatively low level of ab initio theory employed likely contributes to this discrepancy as evidenced by the work of Kjaergaard et al.<sup>50</sup> However, full dimensional quantum vibrational calculation of such a complex molecule is not possible, and it is expected that the absorption intensity is mainly given by the O–H stretching chromophore. Thereby, we are confident that the absorption intensities, at least the ratios between the two stretching modes, are accurate for the decomposition of the experimental spectra. There is significant literature evidence that local mode calculations will give good relative intensities even with lower ab initio levels such as Hartree–Fock (HF), B3LYP,

and Møller–Plesset second-order perturbation theory (MP2),<sup>51,52</sup> including molecules with intramolecular hydrogen bonds.<sup>53,54</sup>

The experimental harmonic frequencies and anharmonic constants were extracted from the linear fits in the Birge–Spencer plot (Figure 2). For the acidic O–H stretch ( $\nu_1$ ), the experimentally extracted harmonic frequency ( $\omega_e$ ) and anharmonic constant ( $\omega_e x_e$ ) were found to be 3743.0 and 80.3 cm<sup>-1</sup> respectively. For the alcohol O–H stretch ( $\nu_2$ ), the experimentally extracted values were found to be 3747.7 and 82.2 cm<sup>-1</sup>. These results are summarized in Table 3.

Spectra of glycolic acid taken with a 1% impurity of water (wet sample) showed very different behavior to the sample that

had been prepared by vacuum sublimation (dry). By examining the intensity of the water rotational lines<sup>35</sup> between 13 150 and 13 600  $\text{cm}^{-1}$  in high-resolution spectra (0.01 nm), the wet sample was found to contain an upper limit of 36 Pa of  $\text{H}_2\text{O}$  vapor. Figure 3 shows a representative spectrum obtained under wet conditions. The spectrum contains a broad, weak underlying spectral feature that was absent from dry spectra. Spectra were taken in the wet sample in regions where  $\text{H}_2\text{O}$  and  $\text{O}_2$  vapors absorbed strongly to ensure that this absorbance feature was not caused by these two species directly. Also, a check was made on the absorbance of glycolic acid's thermal decomposition products of  $\text{CH}_2\text{O}$  and  $\text{CO}$  in the region of 13 150–13 600  $\text{cm}^{-1}$  which confirmed that the feature was not a result of the high-temperature decomposition reaction. Thus, this work is confident that the broad spectral feature, while dependent on water partial pressure, is not directly caused by  $\text{H}_2\text{O}$ ,  $\text{O}_2$ ,  $\text{CH}_2\text{O}$ , or  $\text{CO}$ .

Another interesting result was found by examining what happens when dry glycolic acid and wet glycolic acid are allowed to mix. This means that glycolic acid that had been prepared by vacuum sublimation (dry) was allowed to come together with a sample of the acid that had a  $\sim 1\%$  impurity of water (wet) over a time scale of 8 h. Initially, one obtains a spectrum similar to that of Figure 1 after introduction of the dry sample. Over several minutes, the spectrum resembles that shown in Figure 3. Over a period of much longer times (hours), the dry sample spectrum of Figure 1 is observed. This time dependence could be attributed to water being used up by the glycolic acid sample through intermolecular hydrogen bonding and clustering.

Theoretical work provides some insight into the cause of the spectral changes. The wet spectra show that the O–H stretching region has been perturbed. The band shape is changed such that the intensity may in fact shift out of the  $4\nu_1/4\nu_2$  transition region and become spread over the broad underlying spectral feature mentioned above (Figure 3). This change is in good qualitative agreement with ab initio structures of glycolic acid clustered with one to six water molecules.<sup>3,4</sup> The theoretical work shows that water may readily and preferentially bond to the carboxylic acid moiety of glycolic acid. The perturbations in the wet spectra may indicate the presence of glycolic acid bonded to one or more water molecules. In fact, the broad underlying spectral feature is not unlike the intermolecular hydrogen-bonding features observed in vibrational spectra of other intermolecular hydrogen-bonded species.<sup>50,55</sup> Hydrogen bonding may affect vibrational transitions in many different ways including spectral shifts, altering intensities, and changing band shapes. Further studies would be required to determine the extent to which the presence of water affects the  $4\nu_1$  acidic O–H stretch. It is concluded that the behavior of this transition is highly sensitive to the presence of water. However, the literature contains no calculations on the vibrational frequencies of these complexes.

Calculations in the present work build on both the theoretical work of Thakkar, Kassimi, and Hu<sup>4</sup> and the experimental cavity ring-down spectra in the present work. The calculations provide frequencies and intensities of  $\text{CH}_2\text{OHCOOH}-\text{H}_2\text{O}$  for three rotational isomers of glycolic acid to aid in the analysis of observed differences in the wet and dry spectra. The calculations are performed using the double harmonic approximation, which makes use of a harmonic potential curve and linear dipole moment function. A compilation of these calculations and comparison, where applicable, to other literature values is presented in Table 4. The binding energies for the hydrated clusters corrected for the basis set superposition error by the

counterpoise method,<sup>56</sup> along with its zero-point corrected energies are also given in Table 4 (at the geometries optimized without the counterpoise correction). For the lowest energy conformer, the frequency of the hydrogen-bonded water O–H stretch was calculated to be 3673  $\text{cm}^{-1}$ . This is close in frequency to the fundamental harmonic frequencies for  $\nu_1$  and  $\nu_2$  of the glycolic acid monomer. In addition, the intensity of the hydrogen-bonded water O–H stretch was calculated to be enhanced by about a factor of 4 from the asymmetric stretch of  $\text{H}_2\text{O}$  and is at least 3 times as intense as either of glycolic acid's O–H stretches. This provides qualitative support that the broad underlying feature is caused by multiple O–H stretching transitions in a distribution of glycolic acid–water ( $\text{CH}_2\text{OHCOOH}-(\text{H}_2\text{O})_n$ ) species.

## Conclusion

This work has presented the first observation of the  $4\nu_1$  and  $4\nu_2$  O–H stretching transitions in gas-phase glycolic acid using cavity ring-down spectroscopy. The transitions were shown to be separating as was predicted in previous work on the near-IR transitions  $\nu_1/\nu_2$  and  $2\nu_1/2\nu_2$ .<sup>1</sup> The band centers of the transitions were extracted and compared with theoretically predicted positions both new and previously reported.<sup>1</sup> Glycolic acid monomer calculations provided anharmonic O–H stretching frequencies, intensities, and relative energies for the three lowest energy conformers. The alcohol O–H stretch exhibits intramolecular hydrogen bonding which may cause discrepancies between theory and experiment, as expected, while the acidic O–H stretch is in better agreement with the theoretical predictions.

Spectra collected in the presence of water are significantly different from those obtained under dry conditions. Specifically, the  $4\nu_1/4\nu_2$  O–H stretching region was perturbed. However, the perturbation is in good qualitative agreement with theoretical predictions of glycolic acid interacting with up to six water molecules.<sup>3,4</sup> New theoretical calculations in the present work have aided in assignments and understanding spectral perturbations by providing harmonic frequencies, intensities, and relative energies for the  $\text{CH}_2\text{OHCOOH}-\text{H}_2\text{O}$  complex. The presence of a broad low intensity feature under wet conditions is probably hydrogen-bonded O–H stretching vibrations of water in a distribution of complexes ( $\text{CH}_2\text{OHCOOH}-(\text{H}_2\text{O})_n$ ). These results may be significant for understanding the effects of clustering and nucleation in more general types of hydrogen-bonded systems and encourage a continued study of complex ensembles of molecular clusters in an atmospheric context using optical spectroscopy techniques.

**Acknowledgment.** V.V. thanks the NSF for funding. We also acknowledge the support of Academia Sinica and the National Science Council of Taiwan. S. S. Brown is thanked for CRD expertise and support. H. G. Kjaergaard is also thanked for insight and useful discussions.

## References and Notes

- (1) Havey, D. K.; Feierabend, K. J.; Vaida, V. *J. Phys. Chem. A* **2004**, *108*, 9069.
- (2) Hollenstein, H.; Schar, R. W.; Schwizgebel, N.; Grassi, G.; Gunthard, H. H. *Spectrochim. Acta, Part A* **1983**, *39*, 193.
- (3) Roy, A. K.; Hu, S. W.; Thakkar, A. J. *J. Chem. Phys.* **2005**, *122*.
- (4) Thakkar, A. J.; Kassimi, N. E.; Hu, S. W. *Chem. Phys. Lett.* **2004**, *387*, 142.
- (5) Flock, M.; Ramek, M. *Int. J. Quantum Chem.* **1992**, *26*, 505.
- (6) Godfrey, P. D.; Rodgers, F. M.; Brown, R. D. *J. Am. Chem. Soc.* **1997**, *119*, 2232.
- (7) Blom, C. E.; Bauder, A. *J. Am. Chem. Soc.* **1982**, *104*, 2993.

- (8) *Handbook of Data on Common Organic Compounds*; Lide, D. R., Milne, G. W. A., Eds.; CRC Press: Ann Arbor, MI, 1995; Vol. 1.
- (9) Souza, S. R.; Vasconcellos, P. C.; Carvalho, L. R. F. *Atmos. Environ.* **1999**, *33*, 2563.
- (10) Havey, D. K.; Vaida, V. *J. Mol. Spectrosc.* **2004**, *228*, 152.
- (11) Crim, F. F. *Annu. Rev. Phys. Chem.* **1993**, *44*, 397.
- (12) Henry, B. R. *Acc. Chem. Res.* **1987**, *20*, 429.
- (13) Sinha, A.; Vanderwal, R. L.; Crim, F. F. *J. Chem. Phys.* **1989**, *91*, 2929.
- (14) Henry, B. R.; Kjaergaard, H. G. *Can. J. Chem.* **2002**, *80*, 1635.
- (15) Roehl, C. M.; Nizkorodov, S. A.; Zhang, H.; Blake, G. A.; Wennberg, P. O. *J. Phys. Chem. A* **2002**, *106*, 3766.
- (16) Child, M. S.; Halonen, L. *Adv. Chem. Phys.* **1984**, *57*, 1.
- (17) Henry, B. R. *Acc. Chem. Res.* **1977**, *10*, 207.
- (18) Quack, M. *Annu. Rev. Phys. Chem.* **1990**, *41*, 839.
- (19) Halonen, L. Local mode vibrations in polyatomic molecules. In *Advances in Chemical Physics*; 1998; Vol. 104; p 41.
- (20) Jensen, P. *Mol. Phys.* **2000**, *98*, 1253.
- (21) Vaida, V. *Int. J. Photoenergy* **2005**, *7*, 61.
- (22) Mills, M. J.; Toon, O. B.; Vaida, V.; Hintze, P. E.; Kjaergaard, H. G.; Schofield, D. P.; Robinson, T. W. *J. Geophys. Res. [Atmos.]* **2005**, *110*.
- (23) Donaldson, D. J.; Tuck, A. F.; Vaida, V. *Chem. Rev.* **2003**, *103*, 4717.
- (24) Vaida, V.; Kjaergaard, H. G.; Hintze, P. E.; Donaldson, D. J. *Science* **2003**, *299*, 1566.
- (25) Donaldson, D. J.; Tuck, A. F.; Vaida, V. *Phys. Chem. Earth, Part C* **2000**, *25*, 223.
- (26) Frost, G. J.; Ellison, G. B.; Vaida, V. *J. Phys. Chem. A* **1999**, *103*, 10169.
- (27) Donaldson, D. J.; Frost, G. J.; Rosenlof, K. H.; Tuck, A. F.; Vaida, V. *Geophys. Res. Lett.* **1997**, *24*, 2651.
- (28) Brown, S. S.; Wilson, R. W.; Ravishankara, A. R. *J. Phys. Chem. A* **2000**, *104*, 4976.
- (29) Gomes, J. A. G.; Gossage, J. L.; Balu, H.; Kesmez, M.; Bowen, F.; Lumpkin, R. S.; Cocke, D. L. *Spectrochim. Acta, Part A* **2005**, *61*, 3082.
- (30) Kjaergaard, H. G.; Robinson, T. W.; Howard, D. L.; Daniel, J. S.; Headrick, J. E.; Vaida, V. *J. Phys. Chem. A* **2003**, *107*, 10680.
- (31) Vaida, V.; Kjaergaard, H. G.; Feierabend, K. J. *Int. Rev. Phys. Chem.* **2003**, *22*, 203.
- (32) Chuchani, G.; Martin, I.; Rotinov, A.; Dominguez, R. M. *J. Phys. Org. Chem.* **1993**, *6*, 54.
- (33) Jones, R. E.; Templeton, D. H. *Acta Crystallogr.* **1958**, *11*, 484.
- (34) Atkinson, D. B.; Hudgens, J. W. *J. Phys. Chem. A* **1997**, *101*, 3901.
- (35) Rothman, L. S.; Jacquemart, D.; Barbe, A.; Benner, D. C.; Birk, M.; Brown, L. R.; Carleer, M. R.; Chackerian, C.; Chance, K.; Coudert, L. H.; Dana, V.; Devi, V. M.; Flaud, J. M.; Gamache, R. R.; Goldman, A.; Hartmann, J. M.; Jucks, K. W.; Maki, A. G.; Mandin, J. Y.; Massie, S. T.; Orphal, J.; Perrin, A.; Rinsland, C. P.; Smith, M. A. H.; Tennyson, J.; Tolchenov, R. N.; Toth, R. A.; Vander Auwera, J.; Varanasi, P.; Wagner, G. *J. Quant. Spectrosc. Radiat. Transfer* **2005**, *96*, 139.
- (36) Feierabend, K. J.; Havey, D. K.; Brown, S. S.; Vaida, V. *Chem. Phys. Lett.* **2006**, *420*, 443.
- (37) Becke, A. D. *J. Chem. Phys.* **1993**, *98*, 5648.
- (38) Lee, C.; Yang, W.; Parr, R. G. *Phys. Rev. B* **1988**, *37*, 785.
- (39) Clark, T.; Chandrasekhar, J.; Spitznagel, G. W.; Schleyer, P. v. R. *J. Comput. Chem.* **1983**, *4*, 294.
- (40) Frisch, M. J.; Pople, J. A.; Binkley, J. S. *J. Chem. Phys.* **1984**, *80*, 3265.
- (41) Frisch, M. J.; Trucks, G. W.; Schlegel, H. B.; Scuseria, G. E.; Robb, M. A.; Cheeseman, J. R.; Montgomery, J. A., Jr.; Vreven, T.; Kudin, K. N.; Burant, J. C.; Millam, J. M.; Iyengar, S. S.; Tomasi, J.; Barone, V.; Mennucci, B.; Cossi, M.; Scalmani, G.; Rega, N.; Petersson, G. A.; Nakatsuji, H.; Hada, M.; Ehara, M.; Toyota, K.; Fukuda, R.; Hasegawa, J.; Ishida, M.; Nakajima, T.; Honda, Y.; Kitao, O.; Nakai, H.; Klene, M.; Li, X.; Knox, J. E.; Hratchian, H. P.; Cross, J. B.; Adamo, C.; Jaramillo, J.; Gomperts, R.; Stratmann, R. E.; Yazyev, O.; Austin, A. J.; Cammi, R.; Pomelli, C.; Ochterski, J. W.; Ayala, P. Y.; Morokuma, K.; Voth, G. A.; Salvador, P.; Dannenberg, J. J.; Zakrzewski, V. G.; Dapprich, S.; Daniels, A. D.; Strain, M. C.; Farkas, O.; Malick, D. K.; Rabuck, A. D.; Raghavachari, K.; Foresman, J. B.; Ortiz, J. V.; Cui, Q.; Baboul, A. G.; Clifford, S.; Cioslowski, J.; Stefanov, B. B.; Liu, G.; Liashenko, A.; Piskorz, P.; Komaromi, I.; Martin, R. L.; Fox, D. J.; Keith, T.; Al-Laham, M. A.; Peng, C. Y.; Nanayakkara, A.; Challacombe, M.; Gill, P. M. W.; Johnson, B.; Chen, W.; Wong, M. W.; Gonzalez, C.; Pople, J. A. *Gaussian 03*, Revision C.02; Gaussian, Inc.: Wallingford, CT, 2004.
- (42) Krishnan, R.; Binkley, J. S.; Seeger, R.; Pople, J. A. *J. Chem. Phys.* **1980**, *72*, 650.
- (43) McLean, A. D.; Chandler, G. S. *J. Chem. Phys.* **1980**, *72*, 5639.
- (44) Takahashi, K.; Suguwara, M.; Yabushita, S. *J. Phys. Chem. A* **2002**, *106*, 2676.
- (45) Takahashi, K.; Suguwara, M.; Yabushita, S. *J. Phys. Chem. A* **2003**, *107*, 11092.
- (46) Howard, D. L.; Kjaergaard, H. G. *J. Chem. Phys.* **2004**, *121*, 136.
- (47) Rueda, D.; Boyarkin, O. V.; Rizzo, T. R.; Chirokolava, A.; Perry, D. S. *J. Chem. Phys.* **2005**, *122*.
- (48) Kjaergaard, H. G. *J. Phys. Chem. A* **2002**, *106*, 2979.
- (49) Barone, V. *J. Chem. Phys.* **2005**, *122*, #014108.
- (50) Howard, D. L.; Jorgensen, P.; Kjaergaard, H. G. *J. Am. Chem. Soc.* **2005**, *127*, 17096.
- (51) Kjaergaard, H. G.; Henry, B. R. *J. Chem. Phys.* **1992**, *96*, 4841.
- (52) Kjaergaard, H. G.; Henry, B. R. *Mol. Phys.* **1994**, *83*, 1099.
- (53) Kjaergaard, H. G.; Howard, D. L.; Schofield, D. P.; Robinson, T. W.; Ishiuchi, S.; Fujii, M. *J. Phys. Chem. A* **2002**, *106*, 258.
- (54) Robinson, T. W.; Kjaergaard, H. G.; Ishiuchi, S. I.; Shinozaki, M.; Fujii, M. *J. Phys. Chem. A* **2004**, *108*, 4420.
- (55) Eliason, T. L.; Havey, D. K.; Vaida, V. *Chem. Phys. Lett.* **2005**, *402*, 239.
- (56) Boys, S. F.; Bernard, F. *Mol. Phys.* **1970**, *19*, 553.